Research Article
Visualizing Production Surfaces in 3D Diagrams

I. Seidl and M. Sommersguter-Reichmann

Department of Finance, University of Graz, Universitätsstraße 15, G2, 8010 Graz, Austria

Correspondence should be addressed to M. Sommersguter-Reichmann,
margit.sommersguter@uni-graz.at

During the last four decades Data Envelopment Analysis (DEA) has attracted considerable attention in the OR community. Using DEA, the efficiency frontier is constructed based on assumptions concerning the production possibility set rather than a priori defining a functional relationship between inputs and outputs. In this contribution, we propose an algorithm to visualize the efficiency surface in a 3D diagram and to extract isoquants from the efficient hull based on different RTS assumptions which might be particularly helpful for presentation purposes. In doing so, we extend the existing literature which has concentrated on the visualization of production frontiers in 2D diagrams to the visualization of efficient rather than fully efficient hulls in 3D diagrams. Displaying a fully efficient hull, however, does not reflect all properties of the production possibility set as weakly efficient frontier segments are missing.

1. Introduction

Starting with the pioneering work of Farrell and the subsequent publications on nonparametric efficiency measurement (see [1–4]), a considerable number of applied efficiency measurement studies using nonparametric techniques has been found in the scientific literature [5].

Nonparametric efficiency measurement approaches rely on assumptions concerning the production possibility set (PPS) rather than specifying a functional relationship between inputs and outputs to derive a production frontier, thereby offering a new way to efficiency studies and comparisons. Basically, the idea behind nonparametric efficiency measurement is to derive an unknown production frontier based on the analysis of observable input and output data of different decision making units (DMUs). In particular, using nonparametric approaches, the production frontier is constructed as an envelope to the PPS.

The basics of nonparametric efficiency measurement are often illustrated using diagrams to visualize the derivation of the PPS and the resulting production frontier. Many

of these figures are based on the illustration of the production frontier for the single input single output case which, thus, reflects the maximum and thus efficient quantity of the single output that can be produced using a particular quantity of the single input. Extensions cover the visualization of the production possibility frontier for the two inputs single output and the two outputs single input case, respectively. These diagrams represent the efficient combination of two inputs to produce a particular quantity of a single output and the efficient combination of two outputs that can be produced given a particular quantity of a single input. Illustrations of production frontiers in 3D diagrams have been restricted to the portrayal of fully efficient hulls so far [6].

The purpose of this paper is, thus, to provide an algorithm which can be used to display the efficient hull of a set of DMUs in a 3D diagram, comprising fully as well as weakly efficient frontier segments. With the increasing use of DEA techniques, the visualization of the production surface in the two inputs one output case and the two outputs one input case, respectively, might be useful for presentation purposes. Particularly, the derivation of isoquants directly from the production surface using illustrative data sets is considered to be valuable regarding the discussion of results stemming from differing returns to scale (RTS) assumptions. The purpose of the paper, however, is not to minimize computer speed in producing production surfaces in 3D diagrams but to provide an algorithm which can be used to identify the respective production surface inclusive of the isoquants without using LP methods. In doing so, we consider both variable as well as constant RTS assumptions. For illustration purposes, approaches to derive isoquants for different input and output levels in combination with different RTS assumptions from the so-constructed production surface are presented.

Accordingly, the paper is structured as follows. First, we provide a brief introduction into nonparametric efficiency measurement and its underlying assumptions. Next, we present the algorithms suitable to visualize the efficient hull under constant returns to scale (CRS) and variable returns to scale (VRS) for the case of two inputs and one output. Finally, an algorithm to extract isoquants from the efficient hull for different output levels and different RTS assumptions is presented. All algorithms provided in this contribution have been implemented in Matlab. Some concluding remarks are given in the final section.

2. Nonparametric Efficiency Measurement and Frontier Visualization in 2D Diagrams

Nonparametric efficiency measurement is based on the analysis of observable input and output data of different DMUs. These input output correspondences constitute the PPS. To obtain an estimate of the unknown production frontier, particular assumptions concerning the PPS are made.

Consider a multiple input multiple output setting where DMU j uses the input vector $x_j \in \mathbb{R}_+^m$ to produce the output vector $y_j \in \mathbb{R}_+^s$. The set of feasible input output activities (x, y) is called P with the following properties (for a comprehensive discussion see, e.g., [7, page 42]).

(1) All observed activities belong to P, that is, $(x_j, y_j) \in P$, for all $j = 1, \ldots, n$ DMUs.

(2) If activity (x, y) belongs to P, activity (tx, ty) with $t > 0$ belongs to P, through this property we assume CRS, that is, we obtain P^{CRS}.

(3) If activity (x, y) belongs to P, then the activities (x', y'), (x, y'), and (x', y), with $x' \geq x$ and $y \geq y'$, belong to P as well.

(4) P is the smallest closed and bounded set which meets the above assumptions.

Using matrix notation $X = (x_j) \in \mathbb{R}_+^{m \times n}$ and $Y = (y_j) \in \mathbb{R}_+^{s \times n}$, P^{CRS} can be defined as follows:

$$P^{\text{CRS}} = \{(x, y) \mid x \geq X\lambda, \ y \leq Y\lambda, \ \lambda \in \mathbb{R}_+^n, \ \lambda \geq 0\}. \tag{2.1}$$

A VRS technology requires the additional constraint $e\lambda = 1$, with e being a row vector with all elements equaling unity resulting in the following definition of P^{VRS}:

$$P^{\text{VRS}} = \{(x, y) \mid x \geq X\lambda, \ y \leq Y\lambda, \ \lambda \in \mathbb{R}_+^n, \ \lambda \geq 0, \ e\lambda = 1\}. \tag{2.2}$$

There are also other possibilities of constructing a PPS, such as the nonconvex sets stemming from the free disposal hull approach proposed by [8] or the multiplicative approach proposed by [9]. These approaches are, however, beyond the scope of this contribution.

Given the respective PPS, the technical efficiency of a DMU j $(j = 1, \ldots, n)$ can then be assessed by measuring the distance to the frontier. Among the variety of metrics, the oriented equiproportionate are the most frequently used. Assuming CRS, the input-oriented technical efficiency θ of DMU 0 can be evaluated by solving the following linear program:

$$\begin{aligned} \min_{\theta, \lambda} \quad & \theta \\ \text{s.t.} \quad & \theta x_0 - X\lambda \geq 0 \\ & Y\lambda \geq y_0 \\ & \lambda \geq 0. \end{aligned} \tag{2.3}$$

Assuming VRS, it is necessary to add the constraint $e\lambda = 1$.

Given the optimal solution to (2.3), it is possible to distinguish between inefficient, weakly efficient and fully efficient DMUs. Inefficiency occurs in case $\theta^* < 1$, which means that the DMU under evaluation can reduce its input level proportionately while still guaranteeing the given output level. Weak (or radial) efficiency is indicated if $\theta^* = 1$, but some of the slack vectors, that is, input excesses $s^- \in \mathbb{R}^m$, with $s^- = \theta^* x_0 - X\lambda$, and output shortfalls $s^+ \in \mathbb{R}^s$, with $s^+ = Y\lambda - y_0$, are positive. Full (Pareto-Koopmans (see [10, 11])) efficiency of DMU 0 prevails if $\binom{-x_0}{y_0} \geq \binom{-x_k}{y_k}$, for all $k = 1, \ldots, n$, that is, no element of the first vector is smaller than the respective element of the second vector and at least one element of the first vector is larger than the respective element of the second vector. Full efficiency therefore requires weak efficiency, while the reverse is not necessarily true.

Table 1: Data for the single input single output case.

	A	B	C	D	E	F	G	H	I	J	K	L	M	N	O
x_1	9,50	3,75	3,75	5,75	8,25	8,00	11,50	14,50	12,00	6,67	6,25	9,25	8,00	12,50	4,25
y	9,25	2,00	4,50	7,00	8,75	4,00	6,00	9,50	9,50	8,00	2,50	7,50	3,00	8,50	2,50

Table 2: Data for the two inputs single output case.

	A	B	C	D	E	F	G	H	I	J	K	L	M	N	O
x_1	9,50	3,75	3,75	5,75	8,25	8,00	11,50	14,50	12,00	6,67	6,25	9,25	8,00	12,50	4,25
x_2	2,50	0,20	2,50	3,00	3,00	0,08	2,50	2,00	4,00	5,00	0,05	1,25	0,50	0,75	0,10
y	9,25	2,00	4,50	7,00	8,75	4,00	6,00	9,50	9,50	8,00	2,50	7,50	3,00	8,50	2,50

Computationally, the difference between weak and full efficiency is obtained in a two-step procedure. First we solve (2.3) to obtain θ^*. Second, using the optimal solution θ^* from (2.3), we solve the following LP:

$$\begin{aligned} \max_{s^-,s^+,\lambda} \quad & es^- + es^+ \\ \text{s.t.} \quad & s^- = \theta^* x_0 - X\lambda \\ & s^+ = Y\lambda - y_0 \\ & \lambda \geq 0; \quad s^- \geq 0; \quad s^+ \geq 0. \end{aligned} \qquad (2.4)$$

In doing so, we obtain the optimal solution (s^{-*}, s^{+*}) which indicates full efficiency if $\theta^* = 1$ and $s^{-*} = 0 \wedge s^{+*} = 0$.

According to the above definitions of inefficient, weakly and fully efficient DMUs, we can therefore identify three different areas of the PPS: inefficient DMUs lie inside the PPS, weakly and fully efficient DMUs are located on the frontier. To differentiate between weakly and fully efficient DMUs, it is necessary to further distinguish between weakly and fully efficient frontier segments. On fully efficient frontier segments, it is not possible to improve any input or output without worsening some other input or output, while, on weakly efficient frontier segments, it is possible to improve an input or output without worsening other input or output.

It is common to visualize the PPS and the resulting frontier, especially the differences between the two frontier segments, in 2D diagrams. We start accordingly with a VRS frontier based on the observation of 15 DMUs that use one input (x_1) to produce a single output (y). Data are summarised in Table 1.

The resulting frontier in the input output space is the envelope to the smallest convex set containing the activities of all 15 DMUs (see Figure 1). DMUs B, C, D, J, E, A, I, and H are located on the frontier and are therefore at least weakly efficient. The remaining DMUs inside the PPS are inefficient. Among the DMUs on the frontier, C, D, J, E, A, and I are fully efficient as they have $\theta^* = 1$, $s^{-*} = 0$, and $s^{+*} = 0$. The other two efficient DMUs on the frontier, B and H, however, are obviously dominated by DMUs C and I, respectively, as B uses the same input quantity to produce less output than C and H uses more input to produce the same level of output than I, that is, B shows positive output slack and H has positive input slack.

Adding a second input x_2 (see Table 2), it is possible to illustrate the difference between proportionate and nonproportionate input changes by computing the single factor
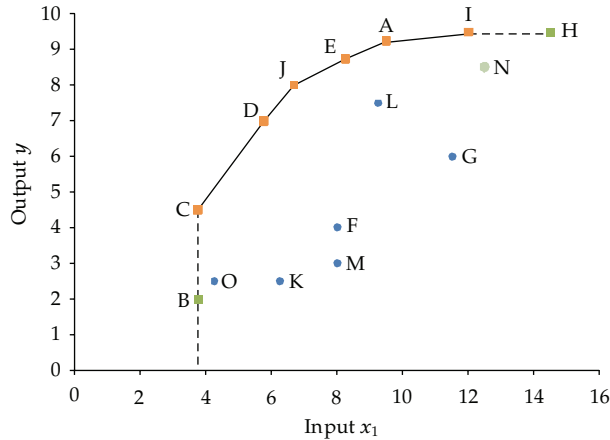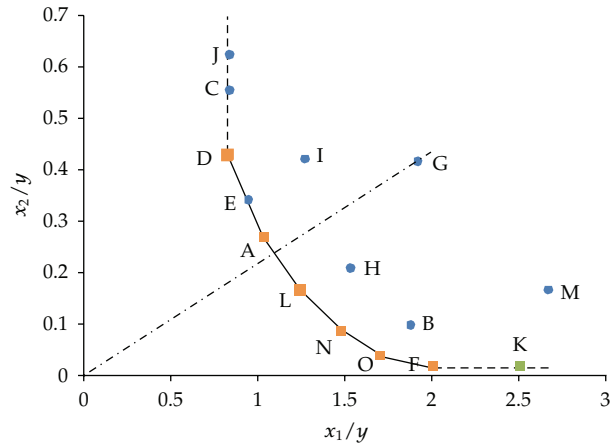
Figure 1: Single input single output case, VRS.

Figure 2: Two inputs single output case, CRS.

productivities x_1/y and x_2/y and depicting the implicitly derived P^{CRS} in the input input space (see Figure 2).

The fully efficient DMUs are now D, A, L, N, O, and F. Among the inefficient DMUs, we find DMU G which obviously has to reduce its inputs proportionately to be located on the frontier. DMU K, however, is now revealed as being weakly efficient, that is, DMU K has no possibility of proportionately reducing its inputs without reducing the output. DMU K, however, uses the same level of input x_2 as DMU F to produce one unit of output y but employs a larger quantity of input x_1 compared to DMU F. For DMU K, a nonproportionate reduction in input x_1 is necessary to produce fully efficient, that is, DMU K shows positive input slack for input x_1, $(s_1^{-*} > 0)$. In contrast to DMU K, the DMUs C, and J, lie slightly inside P^{CRS}. Projecting the DMUs C and J onto the frontier using the input-oriented approach reveals both the necessary proportionate reduction in inputs x_1 and x_2 as well as a nonproportionate reduction in input x_2 as these DMUs are projected onto a weakly efficient segment of the frontier.
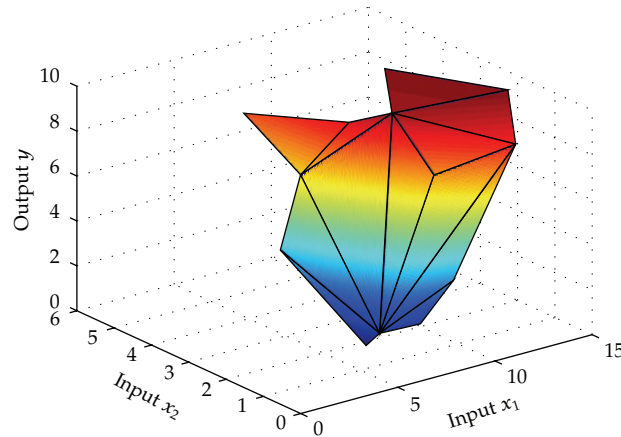
Figure 3: Fully efficient hull.

Obviously, in the case of two inputs and one output, most illustrations fall back on isoquants to explain and visualize how nonparametric efficiency measurement works. Dividing input x_1 and x_2 by the respective output quantity y, however, we implicitly assume CRS and derive an isoquant which does not reflect the prior VRS assumption. An exemption is provided by [12] who illustrate isoquants based on different RTS and disposability assumptions. Overall, isoquants assuming VRS are rarely found as they cannot be constructed as straightforward as under CRS.

Nevertheless, there has been little attempt to visualize the idea behind nonparametric efficiency measurement using production surfaces in 3D diagrams as illustrations of production surfaces in 3D diagrams are hardly found in the literature. If at all, these production surfaces have been restricted to the presentation of fully efficient hulls, similar to those provided in [6], and reproduced in Figure 3 using the data provided in Table 2. Our attempt, however, is to provide an algorithm which can be used to visualize the production surface as an efficient hull (as indicated in Figure 4) with all the properties in (2.1) being visualized. Based on the derivation of the production surface in a 3D diagram, we also propose an algorithm suitable to derive the isoquant under CRS and VRS directly from the efficient hull.

3. Nonparametric Efficiency Measurement and Frontier Visualization in 3D Diagrams

Visualizing the idea behind nonparametric efficiency measurement in 3D diagrams with a fully efficient hull as in Figure 3 does not reflect all properties of the PPS as introduced in (2.1). References [13–15], however, provided algorithms to identify the so-called *strong defining hyperplanes* as well as *weak defining hyperplanes* for the general case of m inputs and s outputs with strong defining hyperplanes corresponding to *fully efficient hyperplanes* and weak defining hyperplanes corresponding to *weakly efficient hyperplanes* according to the terminology used in this contribution. Even though the [13–15] algorithms cover the general case, as far as we know, it has not yet been used to visualize the efficient hull in 3D diagrams. The [13–15] algorithms require the solution to (2.3). The algorithm provided in [16], however, presumes solving (2.3) as well.
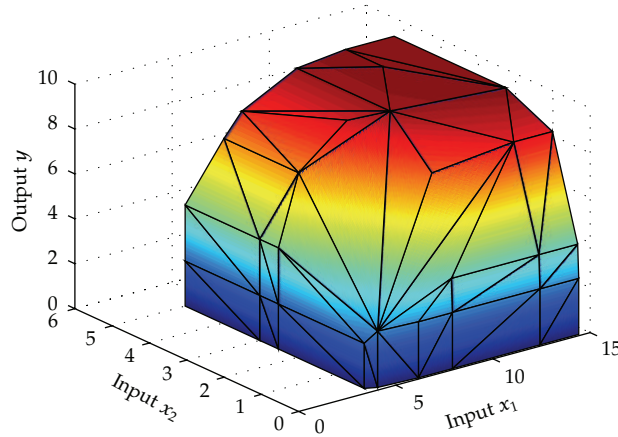
Figure 4: Efficient hull.

The main idea of our first algorithm is to display the efficient hull in a 3D diagram for a set of DMUs that produce a single output with two inputs with the PPS satisfying all properties in (2.1). For the time being, we consider VRS only.

Accordingly, we proceed as follows. First, we show that the fully efficient hull for a set of DMUs is part of the convex hull of the same set. To derive the convex hull, we fall back on the well known Quickhull algorithm (see [17]) rather than solving (2.3) as Quickhull is computationally efficient in producing a convex hull in 3D diagrams. In a second step, we construct the weakly efficient hull falling back, among others, to Quickhull. Finally, we combine the fully and weakly efficient hull to obtain what we call the efficient hull.

3.1. General Remarks

Definition 3.1 (Convex hull). The convex hull S for a set of points Z in a vector space over $\mathbb{R}$ is the minimal convex set containing Z, that is,

$$S(Z) = \left\{ \sum_{i=1}^{k} \alpha_i z_i \mid z_i \in Z, \ \alpha_i \in \mathbb{R}, \ \alpha_i \geq 0, \sum_{i=1}^{k} \alpha_i = 1 \right\}. \tag{3.1}$$

Definition 3.2 (Hyperplane). Hyperplane H in $\mathbb{R}^n$ is a set of the form $\{z \mid pz = k\}$, where p is a nonzero vector in $\mathbb{R}^n$ and k is a scalar. p is usually called normal or gradient to H. H divides $\mathbb{R}^n$ into two halfspaces, H^+ and H^-. H^+ and H^- are two sets of points of the form $\{z \mid pz \geq k\}$ and $\{z \mid pz \leq k\}$, with $H = H^+ \cap H^-$. This definition has been provided in [18].

Based on the above definitions, we can state the following.

Theorem 3.3. *A fully efficient DMU according to* (2.3) *is an element of S.*

Proof. Without loss of generality, we assume that DMU l is fully efficient and not part of S. Consequently, there are two cases.

(a) DMU l is outside S.

(b) DMU l is inside S.

Ad (a): If DMU l is outside S, we have a contradiction to the definition of a convex hull as the minimum convex set containing all DMUs.

Ad (b): If DMU l is inside S, there is a hyperplane of S supported by $m + s$ DMUs. Let DMU f be a convex combination of the $m + s$ DMUs (the so-called virtual DMU) on that hyperplane of S with $y_l \leq y_f \wedge x_l \geq x_f$ and the inequality sign be strict in at least one component. In this case, DMU f dominates DMU l which is a contradiction to the fact that DMU l is fully efficient. $\qquad\qquad\qquad\qquad\qquad\qquad\qquad\qquad\qquad\qquad\qquad\qquad\quad$ □

Definition 3.4 (Fully efficient hull). The fully efficient hull is part of the convex hull. The hyperplanes that constitute the fully efficient hull are called fully efficient hyperplanes H^f. Fully efficient hyperplanes support at least $m + s$ fully efficient DMUs according to (2.3), with negative normal vector components regarding the output vector and positive normal vector components regarding the input vector (see [13]).

Definition 3.5 (Weakly efficient hull). The hyperplanes that constitute the weakly efficient hull are called weakly efficient hyperplanes H^w. Weakly efficient hyperplanes support at least $m + s - 1$ fully efficient DMUs and at least one weakly efficient DMU according to (2.3). The normal vector components concerning the output vector are nonnegative, and the normal vector components concerning the input vector are nonpositive with at least one component of the input or output vector being equal to zero.

Definition 3.6 (Efficient hull). The efficient hull is the combination of the fully and weakly efficient hull.

3.2. Algorithm 1: Producing the Efficient Hull in a 3D Diagram

Based on the definitions in Section 3.1, we now proceed to the description of algorithm 1_VRS which can be used to produce the efficient hull for n DMUs using $m = 2$ inputs to produce $s = 1$ output in a 3D diagram, still assuming VRS.

Step 1. Compute the convex hull with Quickhull. Identify all triangles (Quickhull uses triangles to produce the convex hull in 3D) with normal vector components $x_1 < 0 \wedge x_2 < 0 \wedge y > 0$, and delete all other triangles.

Step 2. Each triangle consists of three vectors. Project the remaining triangles to the x_1x_2-plane with $y = 0$, and delete all vectors which exist two times (inside the 2D hull).

Step 3. Assign the remaining vectors to one of the following groups according to the subsequent procedure.

Start with the minimum output DMU, and go clockwise up to the first vector with normal vector components $x_1 \geq 0 \wedge x_2 > 0$; return to the minimum output DMU; go anticlockwise up to the first vector with normal vector components $x_1 > 0 \wedge x_2 \geq 0$. Concerning the vectors within this range, proceed as follows.

    (a) Vectors with normal vector components $x_1 < 0 \wedge x_2 < 0$ are projected to the x_1x_2-plane with $y = 0$.

(b) Vectors with normal vector components $x_1 \geq 0 \wedge x_2 < 0$ are projected to the $x_2 y$-plane with $x_1 = \max(\text{DMU}_j(x_1))$, $j = 1, \ldots, n$, first, followed by the projection to the $x_1 x_2$-plane with $y = 0$.

(c) Vectors with normal vector components $x_1 < 0 \wedge x_2 \geq 0$ are projected to the $x_1 y$-plane with $x_2 = \max(\text{DMU}_j(x_2))$, $j = 1, \ldots, n$, first, followed by the projection to the $x_1 x_2$-plane with $y = 0$.

Step 4. Go to the maximum output DMU, and go clockwise up to the first vector which has already been assigned to one of the groups 3(a), 3(b), or 3(c) in Step 3. Return to the maximum output DMU, and go anticlockwise up to the first vector which has already been assigned to one of the groups 3(a), 3(b), or 3(c) in Step 3. Concerning the vectors within this range, proceed as follows

(a) clockwise direction: project the vectors between the maximum output DMU and the first vector which has already been assigned to one of the above groups 3(a), 3(b), or 3(c) to the $x_2 y$-plane with $x_1 = \max(\text{DMU}_j(x_1))$, $j = 1, \ldots, n$;

(b) anticlockwise direction: project the vectors between the maximum output DMU and the first vector which has already been assigned to one of the above groups 3(a), 3(b), or 3(c) to the $x_1 y$-plane with $x_2 = \max(\text{DMU}_j(x_2))$, $j = 1, \ldots, n$.

Step 5. Produce the efficient hull in a 3D diagram.

To visualize algorithm 1_VRS, we display some intermediate results graphically. Using Quickhull, the convex hull assuming VRS for the set of 15 DMUs is displayed in Figure 5. Next, the triangles with normal vector components that do not meet the conditions $x_1 < 0 \wedge x_2 < 0 \wedge y > 0$ are deleted. The resulting part is displayed in Figure 6. According to Step 2, the remaining triangles are projected onto the $x_1 x_2$-plane with $y = 0$ as presented in Figure 7. The vectors inside the 2D hull have already been deleted. The minimum (maximum) output DMU is indicated by the solid (dotted) arrow in Figure 7. In accordance with Step 3, we start with the minimum output DMU and go clockwise along the B and A vectors up to the first D vector which has normal vector components $x_1 \geq 0 \wedge x_2 > 0$. Then, we return to the minimum output DMU, and go anticlockwise along the C vectors up to the first D vector with the normal vector components $x_1 > 0 \wedge x_2 \geq 0$. The vectors within this range comprise the A vectors with normal vector components $x_1 < 0 \wedge x_2 \geq 0$ which are thus projected to the $x_1 y$-plane with $x_2 = \max(\text{DMU}_j(x_2))$, $j = 1, \ldots, n$, first, followed by the projection to the $x_1 x_2$-plane with $y = 0$, the two B vectors with normal vector components $x_1 < 0 \wedge x_2 < 0$ which are projected to the $x_1 x_2$-plane with $y = 0$, and, finally, the three C vectors with normal vector components $x_1 \geq 0 \wedge x_2 < 0$ which are projected to the $x_2 y$-plane with $x_1 = \max(\text{DMU}_j(x_1))$, $j = 1, \ldots, n$, followed by a projection to the $x_1 x_2$-plane with $y = 0$. Following Step 4, we now proceed to the maximum output DMU and go clockwise up to the first vector which has already been assigned to one of the groups 3(a), 3(b), or 3(c). As can be seen from Figure 7, this range is empty so that we remain at the maximum output DMU, that is, the projection to the $x_2 y$-plane with $x_1 = \max(\text{DMU}_j(x_1))$, $j = 1, \ldots, n$ is not necessary in this case. Then, we return to the maximum output DMU and go anticlockwise, in this case along the four D vectors up to the A vector. Within this range, the D vectors are projected onto the $x_1 y$-plane with $x_2 = \max(\text{DMU}_j(x_2))$, $j = 1, \ldots, n$. Figure 8 visualizes the resulting efficient hull, using the same letters as in Figure 7 to facilitate comparisons between the hull
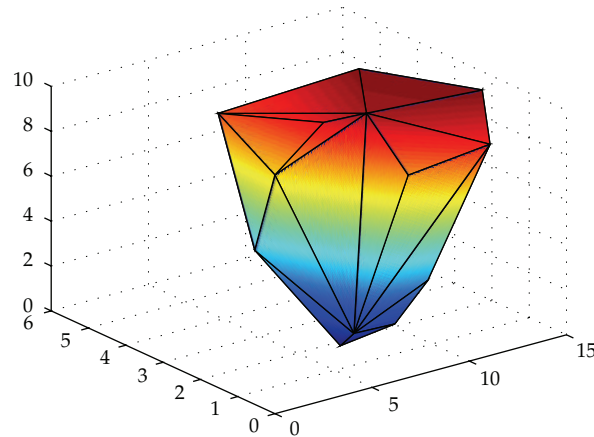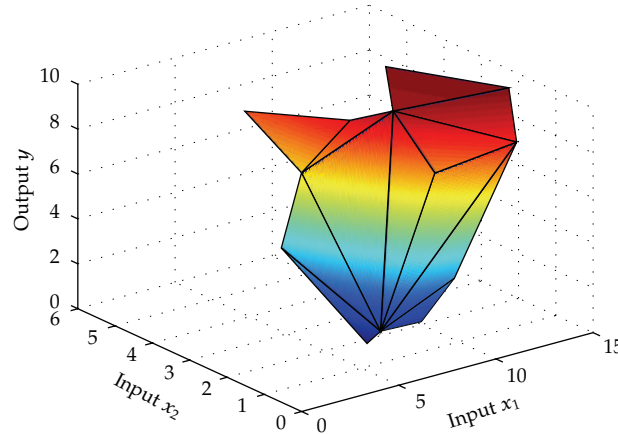
Figure 5: Convex hull, VRS.

Figure 6: Fully efficient hull, VRS.

in the 2D diagram and the hull in the 3D diagram. In Step 5, the efficient hull is produced and displayed in Figure 9.

To take CRS into consideration, we add the origin to the set of DMUs before we proceed with the following Algorithm 1_CRS.

Step 1. Find the maximum x_1x_2-vector, defined as the vector with the components $x_1 = \max(\mathrm{DMU}_j(x_1))$, $j = 1,\ldots,n$, and $x_2 = \max(\mathrm{DMU}_j(x_2))$, $j = 1,\ldots,n$, and compute the unity normal vector for each DMU vector and for the maximum x_1x_2-vector. Step 1 is for illustration purposes only, that is, to obtain a production surface which envelopes all DMUs.

Step 2. Compare the unity normal vector of each DMU vector with the unity normal vector of the maximum x_1x_2-vector, and proceed as follows.

   (a) If the unity normal vector component x_1 of the DMU vector is smaller than the unity normal vector component x_1 of the maximum x_1x_2-vector, then scale the respective DMU vector up to the plane parallel to the x_1y-plane with $x_2 = \max(\mathrm{DMU}_j(x_2))$, $j = 1,\ldots,n$.
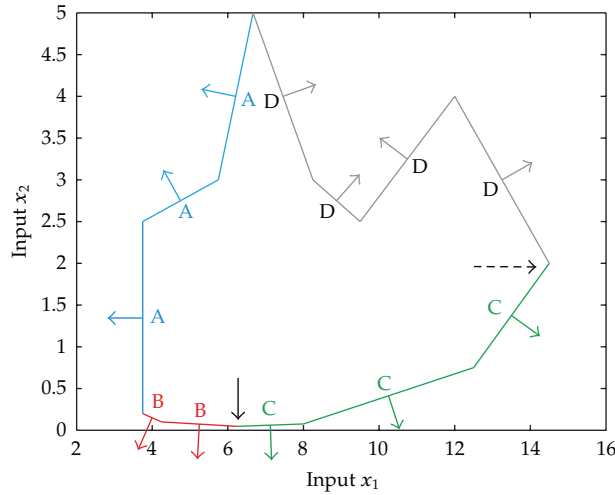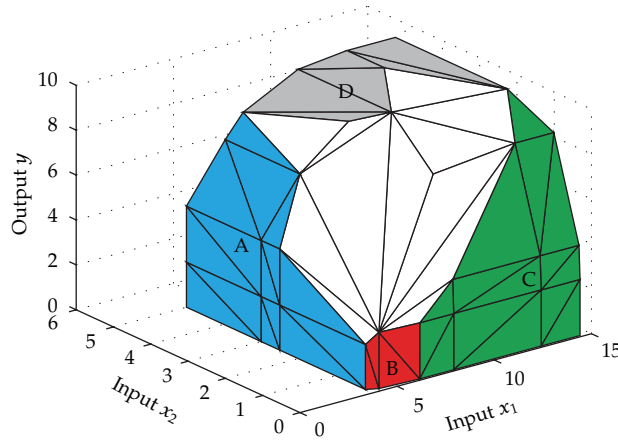
Figure 7: 2D hull.

Figure 8: Efficient hull, VRS.

(b) If the unity normal vector component x_1 of the DMU vector is larger than the unity normal vector component x_1 of the maximum x_1x_2-vector, then scale the respective DMU vector up to the plane parallel to the x_2y-plane with $x_1 = \max(\text{DMU}_j(x_1))$, $j = 1, \ldots, n$.

Step 3. Compute the convex hull with Quickhull for these vectors. Identify all triangles with normal vector components $x_1 \leq 0 \wedge x_2 \leq 0 \wedge y \geq 0$, and delete all other triangles.

Step 4. Project the remaining triangles to the x_1x_2-plane with $y = 0$, save the y-values in a separate list, and delete all vectors

(a) inside the 2D hull and

(b) with normal vector components $x_1 > 0 \wedge x_2 > 0$.

Step 5. Divide the remaining two vectors according to the type of the normal vector into the x_2-vector, adjacent to the x_2-axis (i.e., with normal vector components $x_1 < 0 \wedge x_2 > 0$), and the x_1-vector, adjacent to the x_1-axis (i.e., with normal vector components $x_1 > 0 \wedge x_2 < 0$).

Step 6. Add two new triangles by joining
   (a) the origin (0,0,0), the point $(0, x_2 = \max(\mathrm{DMU}_j(x_2)), j = 1,\dots,n,0)$, and the x_2-vector, inclusive the respective y-value saved according to Step 3;
   (b) the origin (0,0,0), the point $(x_1 = \max(\mathrm{DMU}_j(x_1)), j = 1,\dots,n,0,0)$, and the x_1-vector, inclusive the respective y-value saved according to Step 3.

Step 7. Produce the efficient hull in a 3D diagram.

Figure 10 illustrates the result of Step 3. As we can see, each DMU vector is scaled up to the maximum of x_1 and x_2, respectively, depending on whether the unity normal vector component x_1 of the respective DMU vector is smaller or larger than the unity normal vector component x_1 of the maximum $x_1 x_2$-vector. The triangles with normal vector components $x_1 \leq 0 \wedge x_2 \leq 0 \wedge y \geq 0$ have already been deleted. In addition, Figure 10 reveals that the so-derived part of the efficient hull consists of six different segments, including one weakly efficient segment displayed as the triangle labeled B. This result is consistent with the CRS isoquant portrayed in Figure 2 which consists of five fully efficient isoquant segments. In Figure 11, we provide the results concerning the projection of the remaining triangles to the $x_1 x_2$-plane with $y = 0$ and the deletion of the vectors inside the 2D hull and with normal vector components $x_1 > 0 \wedge x_2 > 0$. According to Step 5, we can identify the A vector as the x_2-vector as it is adjacent to the x_2-axis and the B vector as the x_1-vector as it is adjacent to the x_1-axis. According to Step 6, we now add two new triangles, one by joining the origin (0,0,0), $(0, x_2 = \max(\mathrm{DMU}_j(x_2)), j = 1,\dots,n,0)$ and the x_2-vector as defined in Step 6(a) and the other by joining the origin (0,0,0), $(x_1 = \max(\mathrm{DMU}_j(x_1)), j = 1,\dots,n,0,0)$ and the x_1-vector as defined in Step 6(b). The weakly efficient hull is indicated by the A and the two B triangles in Figure 12. The resulting efficient hull is finally reproduced in Figure 13.

3.3. Algorithm 2: Producing Isoquants in a 2D Diagram

After having constructed the efficient hull for a set of DMUs using Algorithms 1_VRS and 1_CRS, respectively, we now proceed to the illustration of the extraction of the resulting isoquants for different output levels under different RTS assumptions. In doing so, we proceed as follows according to Algorithm 2.

Step 1. Define L as the level of the isoquant to be displayed.

Step 2. Cut off the efficient hull as obtained from Algorithm 1_VRS and/or 1_CRS at level L by identifying all intersecting triangles of the efficient hull. Intersecting triangles are triangles where

   (a) at least one vertex satisfies $y > L$ with the other two vertices satisfying $y \leq L$ or
   (b) at least one vertex satisfies $y < L$ with the other two vertices satisfying $y \geq L$.

Step 3. For each intersecting triangle, compute the two intersection points at level L.
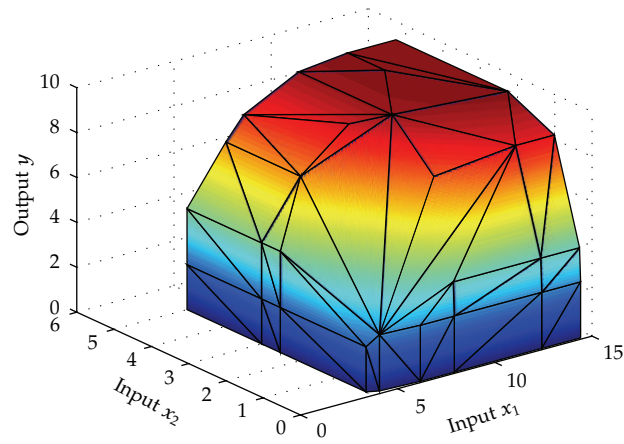
Step 4. Display the isoquant(s) in a 2D diagram.
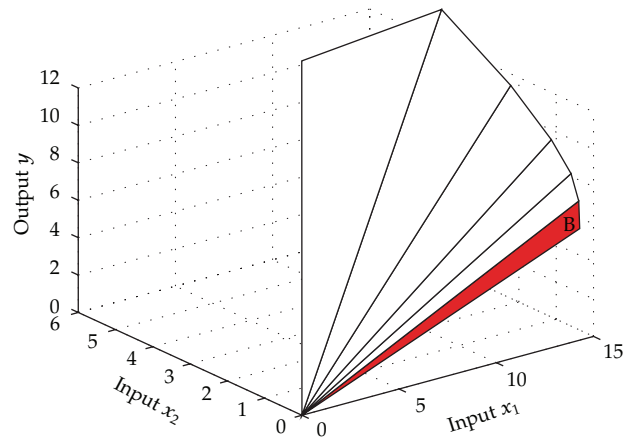
Figure 9: Efficient hull, VRS.
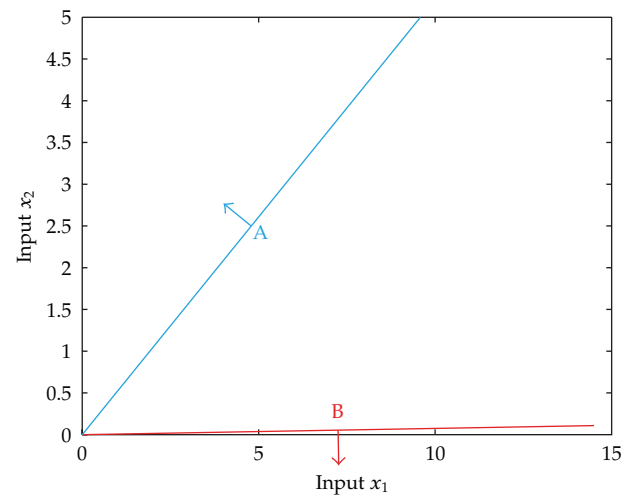

Figure 10: Scaled-up triangles, CRS.

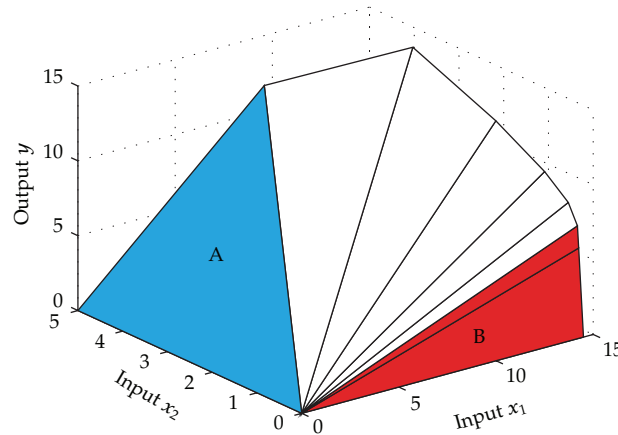**Figure 11:** x_1 and x_2 vector in 2D.

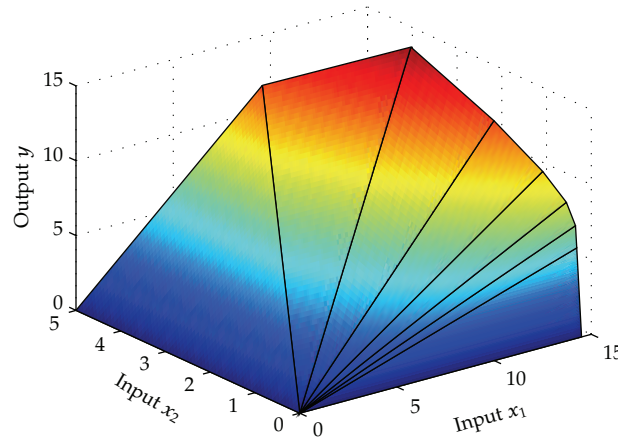**Figure 12:** Fully and all weakly efficient triangles.

Figure 13: Efficient hull, CRS.

Following Algorithm 2, we now display four different isoquants, one for the output level $y = 1$ under VRS and CRS (see Figure 14) as well as for the output level $y = 2,5$ assuming VRS and CRS (see Figure 15). As can be seen from Figure 14, the CRS isoquant in the interval $[2,5;0,5]$ seems smooth rather than piecewise linear in contrast to the isoquant portrayed in Figure 2. For that reason, we enlarge that particular interval for the CRS isoquant to facilitate comparisons. As can be seen in Figure 16, the relevant isoquant consists of seven piecewise linear segments in correspondence with the isoquant displayed in Figure 2.

The algorithms introduced above can also be used to visualize the derivation of output isoquants given the two outputs one input case as illustrated in Figure 17.

4. Concluding Remarks

Deriving a production frontier based on assumptions concerning the production possibility set rather than a priori specifying a functional relationship between inputs and outputs to
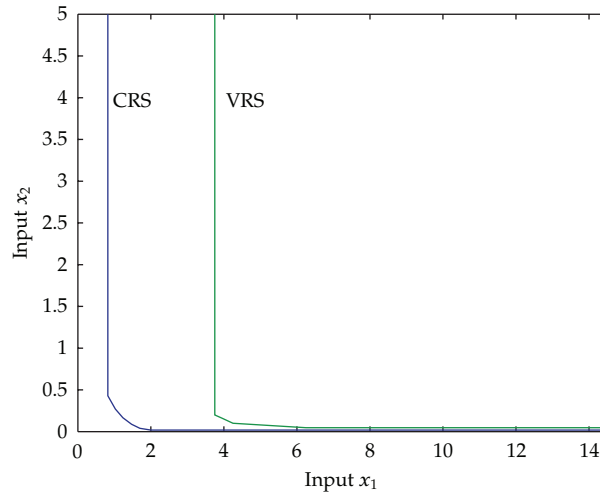
Figure 14: Input isoquants at $y = 1$.
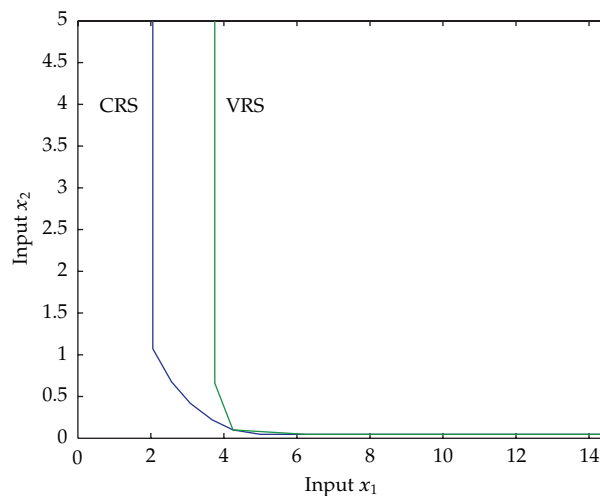
Figure 15: Input isoquants at $y = 2, 5$.

perform efficiency comparisons among different DMUs has attracted considerable attention during the last decades. Most of the ideas inherent in nonparametric efficiency measurement, as well as the results of nonparametric efficiency measurement, have been explained using different types of curves, mostly restricted to illustrations in 2D diagrams. In this contribution, we present algorithms which can be used to determine and visualize a production frontier in the form of an efficient hull in a 3D diagram in the case where multiple DMUs use two inputs to produce a single output. The algorithms introduced can easily be adjusted to the two outputs single input case. In deriving efficient production surfaces for the case of CRS as well as VRS, we fall back on the Quickhull algorithm rather than solving a DEA model. Additionally, based on the so-constructed hulls, we introduce an algorithm to directly derive isoquants for particular output (input) levels and CRS and VRS as well. The
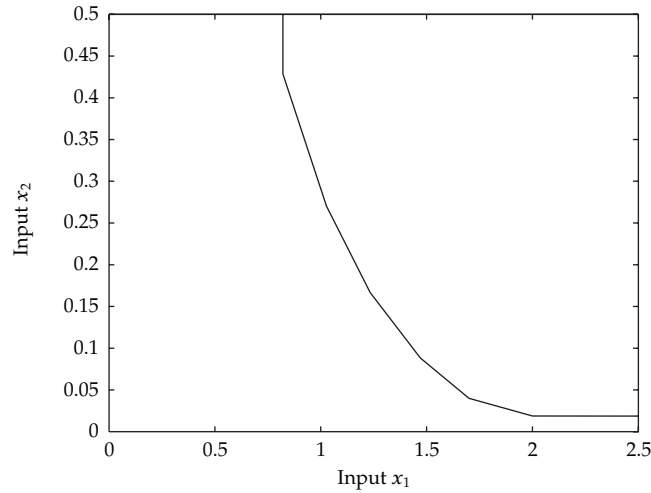
Figure 16: Input isoquant CRS at $y = 1$, enlarged in the interval $[2, 5; 0, 5]$.
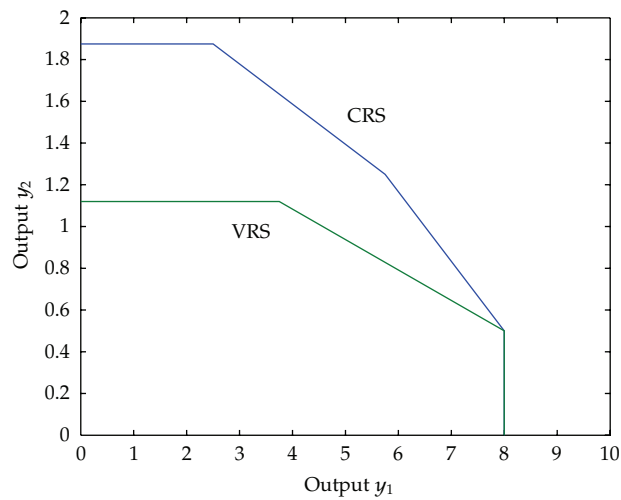

Figure 17: Output isoquants at $x = 3$.

next steps could be the implementation of the above algorithms in available DEA software programs and the optimization of computer speed in producing efficient production surfaces and isoquants.

References

[1] M. J. Farrell, "The measurement of productive efficiency," *Journal of the Royal Statistical Society A*, vol. 120, pp. 253–281, 1957.

[2] A. Charnes, W. W. Cooper, and E. Rhodes, "Measuring the efficiency of decision making units," *European Journal of Operational Research*, vol. 2, no. 6, pp. 429–444, 1978.

[3] R. Färe, S. Grosskopf, and J. Logan, "The relative efficiency of Illinois electric utilities," *Resources and Energy*, vol. 5, no. 4, pp. 349–367, 1983.

[4] R. D. Banker, A. Charnes, and W. W. Cooper, "Some models for estimating technical and scale inefficiencies in data envelopment analysis," *Management Science*, vol. 30, no. 9, pp. 1078–1093, 1984.

[5] L. M. Seiford, "A cyber-bibliography for data envelopment analysis (1978–1999)," in *Data Envelopment Analysis: A Comprehensive Text with Models, Applications, References and DEA-Solver Software*, W. W. Cooper, L. M. Seiford, and K. Tone, Eds., CD-Rom, London, UK, 2000.

[6] A. Ali and L. M. Seiford, "The mathematical programming approach to efficiency analysis," in *The Measurement of Productive Efficiency*, H. O. Fried, C. A. K. Lovell, and S. S. Schmidt, Eds., pp. 120–159, Oxford University Press, Oxford, UK, 1993.

[7] W. W. Cooper, L. M. Seiford, and K. Tone, *Data Envelopment Analysis. A Comprehensive Text with Models, Applications, References and DEA-Solver Software*, London, UK, 2000.

[8] D. Deprins, L. Simar, and H. Tulkens, "Measuring labor-efficiency in post offices," in *The Performance of Public Enterprises. Concept and Measurement*, M. Marchand, P. Pestieau, and H. Tulkens, Eds., pp. 243–267, North Holland, Amsterdam, The Netherlands, 1984.

[9] R. D. Banker and A. Maindiratta, "Piecewise loglinear estimation of efficient production surfaces," *Management Science*, vol. 32, no. 1, pp. 126–135, 1986.

[10] T. C. Koopmans, *Activity Analysis of Production and Allocation*, New York, NY, USA, 1951.

[11] G. Debreu, "The coefficient of resource utilization," *Econometrica*, vol. 19, pp. 273–292, 1951.

[12] P. Byrnes and V. Valdmanis, "Analyzing technical and allocative efficiency of hospitals," in *Data Envelopement Analysis Theory, Methodology and Applications*, A. Charnes, W. Cooper, A. Lewin, and L. Seiford, Eds., Kluwer Academic Publishers, 1997.

[13] G. R. Jahanshahloo, F. H. Lotfi, H. Z. Rezai, and F. R. Balf, "Finding strong defining hyperplanes of production possibility set," *European Journal of Operational Research*, vol. 177, no. 1, pp. 42–54, 2007.

[14] G. R. Jahanshahloo, A. Shirzadi, and S. M. Mirdehghan, "Finding strong defining hyperplanes of PPS using multiplier form," *European Journal of Operational Research*, vol. 194, no. 3, pp. 933–938, 2009.

[15] G. R. Jahanshahloo, F. H. Lotfi, and D. Akbarian, "Finding weak defining hyperplanes of PPS of the BCC model," *Applied Mathematical Modelling*, vol. 34, no. 11, pp. 3321–3332, 2010.

[16] I. Seidl, *Data envelopment analysis visualisiert in 3D-diagrammen*, M.S. thesis, Graz, 2008.

[17] C. B. Barber, D. P. Dobkin, and H. Huhdanpaa, "The quickhull algorithm for convex hulls," *ACM Transactions on Mathematical Software*, vol. 22, no. 4, pp. 469–483, 1996.

[18] H. Ranjbar, F. H. Lotfi, M. Mozaffari, and J. Gerami, "Finding defining hyperplanes with variable returns to scale technology," *International Journal of Mathematical Analysis*, vol. 3, no. 19, pp. 943–954, 2009.